

DESY 03-176

12 December, 2003

Bose-Einstein correlations in one and two dimensions in deep inelastic scattering

ZEUS Collaboration

Abstract

Bose-Einstein correlations in one and two dimensions have been studied in deep inelastic ep scattering events measured with the ZEUS detector at HERA using an integrated luminosity of 121 pb^{-1} . The correlations are independent of the virtuality of the exchanged photon, Q^2 , in the range $0.1 < Q^2 < 8000 \text{ GeV}^2$. There is no significant difference between the correlations in the current and target regions of the Breit frame for $Q^2 > 100 \text{ GeV}^2$. The two-dimensional shape of the particle-production source was investigated, and a significant difference between the transverse and the longitudinal dimensions of the source is observed. This difference also shows no Q^2 dependence. The results demonstrate that Bose-Einstein interference, and hence the size of the particle-production source, is insensitive to the hard subprocess.

The ZEUS Collaboration

S. Chekanov, M. Derrick, D. Krakauer, J.H. Loizides¹, S. Magill, S. Miglioranzi¹, B. Musgrave, J. Repond, R. Yoshida

Argonne National Laboratory, Argonne, Illinois 60439-4815, USA ⁿ

M.C.K. Mattingly

Andrews University, Berrien Springs, Michigan 49104-0380, USA

P. Antonioli, G. Bari, M. Basile, L. Bellagamba, D. Boscherini, A. Bruni, G. Bruni, G. Cara Romeo, L. Cifarelli, F. Cindolo, A. Contin, M. Corradi, S. De Pasquale, P. Giusti, G. Iacobucci, A. Margotti, A. Montanari, R. Nania, F. Palmonari, A. Pesci, G. Sartorelli, A. Zichichi

University and INFN Bologna, Bologna, Italy ^e

G. Aghuzumtsyan, D. Bartsch, I. Brock, S. Goers, H. Hartmann, E. Hilger, P. Irrgang, H.-P. Jakob, O. Kind, U. Meyer, E. Paul², J. Rautenberg, R. Renner, A. Stifutkin, J. Tandler, K.C. Voss, M. Wang, A. Weber³

Physikalisches Institut der Universität Bonn, Bonn, Germany ^b

D.S. Bailey⁴, N.H. Brook, J.E. Cole, G.P. Heath, T. Namsoo, S. Robins, M. Wing
H.H. Wills Physics Laboratory, University of Bristol, Bristol, United Kingdom ^m

M. Capua, A. Mastroberardino, M. Schioppa, G. Susinno

Calabria University, Physics Department and INFN, Cosenza, Italy ^e

J.Y. Kim, Y.K. Kim, J.H. Lee, I.T. Lim, M.Y. Pac⁵

Chonnam National University, Kwangju, Korea ^g

A. Caldwell⁶, M. Helbich, X. Liu, B. Mellado, Y. Ning, S. Paganis, Z. Ren, W.B. Schmidke, F. Sciulli

Nevis Laboratories, Columbia University, Irvington on Hudson, New York 10027 ^o

J. Chwastowski, A. Eskreys, J. Figiel, A. Galas, K. Olkiewicz, P. Stopa, L. Zawiejski
Institute of Nuclear Physics, Cracow, Poland ⁱ

L. Adamczyk, T. Bold, I. Grabowska-Bołd⁷, D. Kisielewska, A.M. Kowal, M. Kowal, T. Kowalski, M. Przybycień, L. Suszycki, D. Szuba, J. Szuba⁸

Faculty of Physics and Nuclear Techniques, AGH-University of Science and Technology, Cracow, Poland ^p

A. Kotański⁹, W. Słomiński

Department of Physics, Jagellonian University, Cracow, Poland

V. Adler, U. Behrens, I. Bloch, K. Borras, V. Chiochia, D. Dannheim, G. Drews, J. Fourletova, U. Fricke, A. Geiser, P. Göttlicher¹⁰, O. Gutsche, T. Haas, W. Hain, S. Hillert¹¹, B. Kahle, U. Kötz, H. Kowalski¹², G. Kramberger, H. Labes, D. Lelas, H. Lim, B. Löhr, R. Mankel, I.-A. Melzer-Pellmann, C.N. Nguyen, D. Notz, A.E. Nuncio-Quiroz, A. Polini, A. Raval, L. Rurua, U. Schneekloth, U. Stoesslein, G. Wolf, C. Youngman, W. Zeuner
Deutsches Elektronen-Synchrotron DESY, Hamburg, Germany

S. Schlenstedt
DESY Zeuthen, Zeuthen, Germany

G. Barbagli, E. Gallo, C. Genta, P. G. Pelfer
University and INFN, Florence, Italy^e

A. Bamberger, A. Benen, N. Coppola
Fakultät für Physik der Universität Freiburg i.Br., Freiburg i.Br., Germany^b

M. Bell, P.J. Bussey, A.T. Doyle, J. Ferrando, J. Hamilton, S. Hanlon, D.H. Saxon, I.O. Skillicorn
Department of Physics and Astronomy, University of Glasgow, Glasgow, United Kingdom^m

I. Gialas
Department of Engineering in Management and Finance, Univ. of Aegean, Greece

B. Bodmann, T. Carli, U. Holm, K. Klimek, N. Krumnack, E. Lohrmann, M. Milite, H. Salehi, P. Schleper, S. Stonjek¹¹, K. Wick, A. Ziegler, Ar. Ziegler
Hamburg University, Institute of Exp. Physics, Hamburg, Germany^b

C. Collins-Tooth, C. Foudas, R. Gonçalo¹³, K.R. Long, A.D. Tapper
Imperial College London, High Energy Nuclear Physics Group, London, United Kingdom^m

P. Cloth, D. Filges
Forschungszentrum Jülich, Institut für Kernphysik, Jülich, Germany

M. Kataoka¹⁴, K. Nagano, K. Tokushuku¹⁵, S. Yamada, Y. Yamazaki
Institute of Particle and Nuclear Studies, KEK, Tsukuba, Japan^f

A.N. Barakbaev, E.G. Boos, N.S. Pokrovskiy, B.O. Zhautykov
Institute of Physics and Technology of Ministry of Education and Science of Kazakhstan, Almaty, Kazakhstan

D. Son
Kyungpook National University, Center for High Energy Physics, Daegu, South Korea^g

K. Piotrkowski

Institut de Physique Nucléaire, Université Catholique de Louvain, Louvain-la-Neuve, Belgium

F. Barreiro, C. Glasman¹⁶, O. González, L. Labarga, J. del Peso, E. Tassi, J. Terrón, M. Vázquez, M. Zambrana

Departamento de Física Teórica, Universidad Autónoma de Madrid, Madrid, Spain^l

M. Barbi, F. Corriveau, S. Gliga, J. Lainesse, S. Padhi, D.G. Stairs, R. Walsh

Department of Physics, McGill University, Montréal, Québec, Canada H3A 2T8^a

T. Tsurugai

Meiji Gakuin University, Faculty of General Education, Yokohama, Japan^f

A. Antonov, P. Danilov, B.A. Dolgoshein, D. Gladkov, V. Sosnovtsev, S. Suchkov

Moscow Engineering Physics Institute, Moscow, Russia^j

R.K. Dementiev, P.F. Ermolov, Yu.A. Golubkov¹⁷, I.I. Katkov, L.A. Khein, I.A. Korzhavina, V.A. Kuzmin, B.B. Levchenko¹⁸, O.Yu. Lukina, A.S. Proskuryakov, L.M. Shcheglova, N.N. Vlasov¹⁹, S.A. Zotkin

Moscow State University, Institute of Nuclear Physics, Moscow, Russia^k

N. Coppola, S. Grijpink, E. Koffeman, P. Kooijman, E. Maddox, A. Pellegrino, S. Schagen, H. Tiecke, J.J. Velthuis, L. Wiggers, E. de Wolf

NIKHEF and University of Amsterdam, Amsterdam, Netherlands^h

N. Brümmner, B. Bylsma, L.S. Durkin, T.Y. Ling

Physics Department, Ohio State University, Columbus, Ohio 43210ⁿ

A.M. Cooper-Sarkar, A. Cottrell, R.C.E. Devenish, B. Foster, G. Grzelak, C. Gwenlan²⁰, S. Patel, P.B. Straub, R. Walczak

Department of Physics, University of Oxford, Oxford United Kingdom^m

A. Bertolin, R. Brugnera, R. Carlin, F. Dal Corso, S. Dusini, A. Garfagnini, S. Limentani, A. Longhin, A. Parenti, M. Posocco, L. Stanco, M. Turcato

Dipartimento di Fisica dell'Università and INFN, Padova, Italy^e

E.A. Heaphy, F. Metlica, B.Y. Oh, J.J. Whitmore²¹

Department of Physics, Pennsylvania State University, University Park, Pennsylvania 16802^o

Y. Iga

Polytechnic University, Sagamihara, Japan^f

G. D'Agostini, G. Marini, A. Nigro

Dipartimento di Fisica, Università 'La Sapienza' and INFN, Rome, Italy^e

C. Cormack²², J.C. Hart, N.A. McCubbin
Rutherford Appleton Laboratory, Chilton, Didcot, Oxon, United Kingdom^m

C. Heusch
*University of California, Santa Cruz, California 95064, USA*ⁿ

I.H. Park
Department of Physics, Ewha Womans University, Seoul, Korea

N. Pavel
Fachbereich Physik der Universität-Gesamthochschule Siegen, Germany

H. Abramowicz, A. Gabareen, S. Kananov, A. Kreisel, A. Levy
Raymond and Beverly Sackler Faculty of Exact Sciences, School of Physics, Tel-Aviv University, Tel-Aviv, Israel^d

M. Kuze
Department of Physics, Tokyo Institute of Technology, Tokyo, Japan^f

T. Fusayasu, S. Kagawa, T. Kohno, T. Tawara, T. Yamashita
Department of Physics, University of Tokyo, Tokyo, Japan^f

R. Hamatsu, T. Hirose², M. Inuzuka, H. Kaji, S. Kitamura²³, K. Matsuzawa
Tokyo Metropolitan University, Department of Physics, Tokyo, Japan^f

M.I. Ferrero, V. Monaco, R. Sacchi, A. Solano
Università di Torino and INFN, Torino, Italy^e

M. Arneodo, M. Ruspa
Università del Piemonte Orientale, Novara, and INFN, Torino, Italy^e

T. Koop, G.M. Levman, J.F. Martin, A. Mirea
Department of Physics, University of Toronto, Toronto, Ontario, Canada M5S 1A7^a

J.M. Butterworth²⁴, R. Hall-Wilton, T.W. Jones, M.S. Lightwood, M.R. Sutton, C. Targett-Adams
Physics and Astronomy Department, University College London, London, United Kingdom^m

J. Ciborowski²⁵, R. Ciesielski²⁶, P. Łuźniak²⁷, R.J. Nowak, J.M. Pawlak, J. Sztuk²⁸, T. Tymieniecka²⁹, A. Ukleja²⁹, J. Ukleja³⁰, A.F. Żarnecki
Warsaw University, Institute of Experimental Physics, Warsaw, Poland^q

M. Adamus, P. Plucinski
Institute for Nuclear Studies, Warsaw, Poland^q

Y. Eisenberg, L.K. Gladilin³¹, D. Hochman, U. Karshon M. Riveline
Department of Particle Physics, Weizmann Institute, Rehovot, Israel^c

D. Kçira, S. Lammers, L. Li, D.D. Reeder, M. Rosin, A.A. Savin, W.H. Smith
Department of Physics, University of Wisconsin, Madison, Wisconsin 53706, USA ⁿ

A. Deshpande, S. Dhawan
Department of Physics, Yale University, New Haven, Connecticut 06520-8121, USA ⁿ

S. Bhadra, C.D. Catterall, S. Fourletov, G. Hartner, S. Menary, M. Soares, J. Standage
Department of Physics, York University, Ontario, Canada M3J 1P3 ^a

- ¹ also affiliated with University College London, London, UK
- ² retired
- ³ self-employed
- ⁴ PPARC Advanced fellow
- ⁵ now at Dongshin University, Naju, Korea
- ⁶ now at Max-Planck-Institut für Physik, München, Germany
- ⁷ partly supported by Polish Ministry of Scientific Research and Information Technology, grant no. 2P03B 122 25
- ⁸ partly supp. by the Israel Sci. Found. and Min. of Sci., and Polish Min. of Scient. Res. and Inform. Techn., grant no.2P03B12625
- ⁹ supported by the Polish State Committee for Scientific Research, grant no. 2 P03B 09322
- ¹⁰ now at DESY group FEB
- ¹¹ now at Univ. of Oxford, Oxford/UK
- ¹² on leave of absence at Columbia Univ., Nevis Labs., N.Y., US A
- ¹³ now at Royal Holloway University of London, London, UK
- ¹⁴ also at Nara Women's University, Nara, Japan
- ¹⁵ also at University of Tokyo, Tokyo, Japan
- ¹⁶ Ramón y Cajal Fellow
- ¹⁷ now at HERA-B
- ¹⁸ partly supported by the Russian Foundation for Basic Research, grant 02-02-81023
- ¹⁹ now at University of Freiburg, Germany
- ²⁰ PPARC Postdoctoral Research Fellow
- ²¹ on leave of absence at The National Science Foundation, Arlington, VA, USA
- ²² now at Univ. of London, Queen Mary College, London, UK
- ²³ present address: Tokyo Metropolitan University of Health Sciences, Tokyo 116-8551, Japan
- ²⁴ also at University of Hamburg, Alexander von Humboldt Fellow
- ²⁵ also at Łódź University, Poland
- ²⁶ supported by the Polish State Committee for Scientific Research, grant no. 2 P03B 07222
- ²⁷ Łódź University, Poland
- ²⁸ Łódź University, Poland, supported by the KBN grant 2P03B12925
- ²⁹ supported by German Federal Ministry for Education and Research (BMBF), POL 01/043
- ³⁰ supported by the KBN grant 2P03B12725
- ³¹ on leave from MSU, partly supported by University of Wisconsin via the U.S.-Israel BSF

- ^a supported by the Natural Sciences and Engineering Research Council of Canada (NSERC)
- ^b supported by the German Federal Ministry for Education and Research (BMBF), under contract numbers HZ1GUA 2, HZ1GUB 0, HZ1PDA 5, HZ1VFA 5
- ^c supported by the MINERVA Gesellschaft für Forschung GmbH, the Israel Science Foundation, the U.S.-Israel Binational Science Foundation and the Benozio Center for High Energy Physics
- ^d supported by the German-Israeli Foundation and the Israel Science Foundation
- ^e supported by the Italian National Institute for Nuclear Physics (INFN)
- ^f supported by the Japanese Ministry of Education, Culture, Sports, Science and Technology (MEXT) and its grants for Scientific Research
- ^g supported by the Korean Ministry of Education and Korea Science and Engineering Foundation
- ^h supported by the Netherlands Foundation for Research on Matter (FOM)
- ⁱ supported by the Polish State Committee for Scientific Research, grant no. 620/E-77/SPB/DESY/P-03/DZ 117/2003-2005
- ^j partially supported by the German Federal Ministry for Education and Research (BMBF)
- ^k partly supported by the Russian Ministry of Industry, Science and Technology through its grant for Scientific Research on High Energy Physics
- ^l supported by the Spanish Ministry of Education and Science through funds provided by CICYT
- ^m supported by the Particle Physics and Astronomy Research Council, UK
- ⁿ supported by the US Department of Energy
- ^o supported by the US National Science Foundation
- ^p supported by the Polish State Committee for Scientific Research, grant no. 112/E-356/SPUB/DESY/P-03/DZ 116/2003-2005, 2 P03B 13922
- ^q supported by the Polish State Committee for Scientific Research, grant no. 115/E-343/SPUB-M/DESY/P-03/DZ 121/2001-2002, 2 P03B 07022

1 Introduction

The quantum-mechanical wave-function for a pair of identical bosons is symmetric under particle exchange. As a consequence, interference effects are expected between identical bosons emitted close to one another in phase space. These effects enhance the two-particle density at small phase-space separations. Such Bose-Einstein (BE) correlations for like-charged hadrons were first observed by Goldhaber et al. [1] in $\bar{p}p$ annihilation.

The BE correlations in momentum space are related to the spatial dimensions of the production source. Therefore, studies of the BE effect may lead to a better understanding of the structure of the source of the identical bosons. In deep inelastic scattering (DIS), the production volume may depend on the virtuality of the exchanged photon, Q^2 , since the transverse size of the virtual photon decreases with increasing Q^2 . Under this hypothesis, the BE correlations would depend on Q^2 .

Alternatively, the size of the region over which BE correlations take place may be determined only by the soft, or fragmentation, stage of the process. The BE effect is independent of Q^2 if hard scattering and fragmentation factorise. For example, in the Lund fragmentation model [2, 3], no sensitivity to Q^2 is expected, and the BE correlations between identical bosons are a measure of the tension of the colour string between partons.

This paper reports on investigations of the BE correlations in one and two dimensions in neutral current ep DIS, focusing on the dependence of the BE interference on Q^2 . The BE effect in one dimension is measured with a higher precision than previously in ep collisions [4] and over a much wider kinematic range, from $Q^2 \simeq 0.1 \text{ GeV}^2$ to 8000 GeV^2 . The correlations are also studied for the first time in DIS in the current and the target fragmentation regions of the Breit frame [5], which are known to have rather different fragmentation properties [6]. The two-dimensional analysis provides sensitivity to a possible elongation of the source expected in the Lund string model [3].

2 Definition of measured quantities and model predictions

Bose-Einstein correlations are usually parameterised using a Gaussian expression for the normalised two-particle density [7]:

$$R(Q_{12}) = \alpha (1 + \beta Q_{12}) (1 + \lambda e^{-r^2 Q_{12}^2}), \quad (1)$$

where $Q_{12} \equiv \sqrt{-(p_1 - p_2)^2} = \sqrt{M^2 - 4m_{\text{boson}}^2}$ is the Lorentz-invariant momentum difference between the two identical bosons, which is related to the invariant mass, M , of the

two particles with four-momenta p_1 and p_2 and mass m_{boson} . In the present analysis, all charged particles are assumed to be pions. The parameter λ is a measure of the degree of coherence, i.e. the fraction of pairs of identical particles that undergo interference. For a totally coherent emission of pions, $\lambda = 0$, while for an incoherent source, the symmetrisation of the wave function for identical particles leads to $\lambda = 1$. The quantity r is the radius of the production volume, while the phenomenological parameter β is used to take into account any long-distance correlations, and α is a normalisation constant. The Gaussian parameterisation in Eq. (1) is motivated by the assumption that the emitting sources of identical bosons are described by a spherical Gaussian density function.

When the BE correlations are interpreted in terms of the Lund fragmentation model, the correlation strength is related to the string tension. In this case, the correlations should have an approximately exponential shape [2,3], i.e. $\lambda e^{-r^2 Q_{12}^2}$ in Eq. (1) should be replaced by $\lambda' e^{-r' Q_{12}^2}$.

To calculate $R(Q_{12})$, the inclusive two-particle density, $\rho = 1/N \cdot dn_{\text{pairs}}/dQ_{12}$, was used, where n_{pairs} is the number of particle pairs and N is the number of events. The densities were calculated for like-charged particle combinations ($\rho(++ , --)$) and for unlike-charged combinations ($\rho(+ -)$), and the ratio computed as $\xi = \rho(++ , --)/\rho(+ -)$. This technique helps to remove correlations due to the topology and global properties of the events contributing to $\rho(++ , --)$. The quantity ξ contains additional short-range correlations, due to resonance decays (contributing to $\rho(+ -)$), which must also be removed. To reduce such non-BE effects, a Monte Carlo (MC) sample without the BE effect was used to calculate $\xi^{\text{MC,noBE}}$, and non-Bose-Einstein effects were removed by use of the double ratio, $R(Q_{12}) = \xi^{\text{data}}/\xi^{\text{MC,noBE}}$. In this case, it was assumed that the BE effect can be factorised from other types of correlations, and that non-BE correlations are well described by the MC models.

It is also possible to extract the BE parameters by considering pairs of particles from different events as a reference sample (track-mixing method). This method was not used in the current analysis since it is difficult to control the systematic effects arising from Q^2 differences of the events in the sample. Earlier experiments [8,4] have found that values of r extracted with the track-mixing method is systematically smaller than those obtained with the method used here.

Bose-Einstein correlations can be studied in two dimensions. For this, the longitudinally co-moving system (LCMS) [9] is often used, since in this frame the correlations have a convenient interpretation in the Lund-string model. For ep collisions, the LCMS can be defined for each pair of particles with momenta \mathbf{p}_1 and \mathbf{p}_2 as the frame in which the sum of the two momenta, $\mathbf{p}_1 + \mathbf{p}_2$, is perpendicular to the γ^*q axis, as shown in Fig. 1. The three-momentum difference, $\mathbf{Q} = (\mathbf{p}_2 - \mathbf{p}_1)$, can be decomposed in the LCMS into transverse, Q_T , and longitudinal, Q_L , components. The longitudinal direction is aligned

with the direction of motion of the initial parton. Therefore, in the string model, the LCMS is the local rest frame of a string. In this case, the BE effect can be parameterised using the two-dimensional function

$$R(Q_T, Q_L) = \alpha (1 + \beta_t Q_T + \beta_l Q_L) (1 + \lambda e^{-r_T^2 Q_T^2 - r_L^2 Q_L^2}), \quad (2)$$

where r_T and r_L are the transverse and longitudinal size of the boson source. The measurements were done using this parameterisation and the same procedure as for the one-dimensional study.

The Lund model predicts that the longitudinal size of the production source is larger than the transverse one, $r_L > r_T$ [3]. However, the usual implementation of the BE effect in the Lund MC models does not contain such an elongation.

The Breit frame [5], as shown in Fig. 1, allows the separation of the radiation of the outgoing struck quark from the proton remnant. Therefore, this frame can be used to test the sensitivity of the BE effect to different underlying dynamics. All particles with negative p_Z^{Breit} form the current region. These particles are produced by the fragmentation of the struck quark, so that this region is analogous to a single hemisphere of an e^+e^- annihilation event, while the target region is dominated by the softer fragmentation of the proton remnants.

3 Experimental setup

A detailed description of the ZEUS detector can be found elsewhere [10]. A brief outline of the components that are most relevant for this analysis is given below.

Charged particles are tracked in the central tracking detector (CTD) [11], which operates in a magnetic field of 1.43 T provided by a thin superconducting solenoid. The CTD consists of 72 cylindrical drift chamber layers, organized in nine superlayers covering the polar-angle¹ region $15^\circ < \theta < 164^\circ$. The transverse-momentum resolution for full-length tracks is $\sigma(p_T)/p_T = 0.0058p_T \oplus 0.0065 \oplus 0.0014/p_T$, with p_T in GeV.

The high-resolution uranium–scintillator calorimeter (CAL) [12] consists of three parts: the forward (FCAL), the barrel (BCAL) and the rear (RCAL) calorimeters. Each part is subdivided transversely into towers and longitudinally into one electromagnetic section (EMC) and either one (in RCAL) or two (in BCAL and FCAL) hadronic sections

¹ The ZEUS coordinate system is a right-handed Cartesian system, with the Z axis pointing in the proton beam direction, referred to as the “forward direction”, and the X axis pointing left towards the centre of HERA. The coordinate origin is at the nominal interaction point.

(HAC). The smallest subdivision of the calorimeter is called a cell. The CAL energy resolutions, as measured under test-beam conditions, are $\sigma(E)/E = 0.18/\sqrt{E}$ for electrons and $\sigma(E)/E = 0.35/\sqrt{E}$ for hadrons, with E in GeV.

A presampler [13] is mounted in front of FCAL, BCAL and RCAL. It consists of scintillator tiles that detect particles originating from showers in the material between the interaction point and the calorimeter. This information was used to correct the energy of the scattered electron. The position of electrons scattered close to the electron beam direction is determined by a scintillator strip detector (SRTD) [14].

The beam-pipe calorimeter (BPC) [15] was installed 294 cm from the interaction point in order to enhance the acceptance of the ZEUS detector for low- Q^2 events. It is a tungsten-scintillator sampling calorimeter with the front face located at $Z = -293.7$ cm, the centre at $Y = 0.0$, and the inner edge of the active area at $X = 4.4$ cm, as close as possible to the rear beam pipe. The energy resolution as determined in test-beam measurements with 1–6 GeV electrons is $\sigma_E/E = 17\%/\sqrt{E}$, with E in GeV.

4 Data sample

Two data samples were used for the present analysis. The data for $Q^2 > 4 \text{ GeV}^2$ were taken during the 1996-2000 period and correspond to an integrated luminosity of 121 pb^{-1} . The lepton beam energy was 27.6 GeV and the proton beam energy was 820 GeV (1996-1997) or 920 GeV (1998-2000). The second sample consists of low- Q^2 events taken with the BPC. This sample corresponds to 3.9 pb^{-1} taken during 1997.

The kinematic variables Q^2 and Bjorken x were reconstructed using the electron method (denoted by the subscript e), which uses measurements of the energy and angle of the scattered lepton, the double angle (DA) method [16] or the Jacquet-Blondel (JB) method [17].

The scattered-lepton candidate for the region $Q^2 > 4 \text{ GeV}^2$ was identified from the pattern of energy deposits in the CAL [18]. The following requirements were imposed:

- $Q_e^2 > 4 \text{ GeV}^2$;
- $E_{e'} \geq 10 \text{ GeV}$, where $E_{e'}$ is the corrected energy of the scattered lepton measured in the CAL;
- $40 \leq \delta \leq 60 \text{ GeV}$, where $\delta = \sum E_i(1 - \cos \theta_i)$, E_i is the energy of the i th calorimeter cell, θ_i is its polar angle and the sum runs over all cells;
- $y_e \leq 0.95$ and $y_{\text{JB}} \geq 0.04$;
- $|Z_{\text{vertex}}| < 50 \text{ cm}$, where Z_{vertex} is the vertex position determined from the tracks;

- the position of the scattered-lepton candidate in the RCAL was required to be outside a box of ± 14 cm in X and Y .

In total, 6.4 million events were selected.

The low- Q^2 events, selected in the region $0.1 < Q_e^2 < 1.0$ GeV², were reconstructed by identifying energy deposits in BPC consistent with a scattered positron with an energy of least 7 GeV. The positron position at the BPC front face had to lie within the fiducial area, $5.2 < X < 9.3$ cm and $-2.3 < Y < 2.8$ cm. Other cuts are identical to those used for the data sample at $Q^2 > 4$ GeV², except for the y_{JB} cut, which was raised to $y_{\text{JB}} > 0.06$. The reconstruction of the Breit frame and the Q^2 variable were performed using variables calculated with the electron method. In total, about 100000 events were selected.

The measurement uses CTD tracks assigned to the primary event vertex. Tracks were required to pass through at least three CTD superlayers and have transverse momentum $p_T^{\text{lab}} > 150$ MeV. The approximate pseudorapidity range for selected tracks is $|\eta| < 1.75$. To ensure that tracks were well reconstructed, track pairs were required to satisfy $Q_{12} > 0.05$ GeV. In the kinematic region used for this analysis, pions constitute about 81% of the tracks, according to MC expectations.

5 Reconstruction procedure and acceptance correction

The parameters for the BE effect were determined from a fit using either the Gaussian or exponential parameterisation. The reference sample was calculated using unlike-charged pairs, and then the MC was used to remove the effect of resonances, as discussed in Sect. 2. The regions affected by imperfections in the MC simulations of K_S^0 and ρ^0 decays were excluded from the fit.

The measured correlation functions, $R(Q_{12})$ and $R(Q_T, Q_L)$, were corrected for detector effects using a bin-by-bin procedure. The detector correction factor was calculated from MC events as $\xi^{\text{gen}}/\xi^{\text{det}}$, where $\xi^{\text{gen}}(\xi^{\text{det}})$ is the generated (reconstructed) two-particle density $\rho(++ , --)$ divided by $\rho(+ -)$. No cuts were applied on the true MC hadrons. The corrections are close to unity (1.0 ± 0.1), since some detector effects cancel in the ratios of the two-particle densities. Only for the lowest Q_{12} region ($0.05 < Q_{12} < 0.1$ GeV) the correction is as large 1.3-1.4.

Since the generator-level MC events do not have the BE effect, and are used both for the acceptance correction and for the subtraction of resonances, the final result is equivalent to the detector-level measurement in the restricted kinematic region defined by the cuts in Sect. 4. The effect of these cuts, in particular those on track momentum and angle,

depends upon Q^2 , since Q^2 determines the available phase space for particle production. The MC model containing BE correlations was used to estimate the effect of extrapolation to the full phase space available in each Q^2 bin. The effect was found to be small (+3.5% for the BE radii) and Q^2 independent. This model-dependent correction was not included in the final results.

The MC events were generated with the ARIADNE 4.08 model [19] interfaced with HERACLES 4.5.2 [20] using the DJANGO 1.1 program [21] to incorporate first-order electroweak corrections. The generated events were then passed through a full simulation of the detector using GEANT 3.13 [22] and processed with the same reconstruction program as the data. The detector-level MC samples were then selected in the same way as the data.

To simulate hadronisation, ARIADNE employs the PYTHIA 5.7/JETSET 7.4 program [23], which is based on the Lund string model [24]. The BE effect, which is treated as a final-state interaction by redistributing hadron momenta according to a chosen parameterisation, is available as an option in the PYTHIA/JETSET program. The default parameter setting for ARIADNE does not contain the BE effect. For systematic checks, the BE correlations were included in the simulation for the acceptance calculations. The BE effect was parameterised by a Gaussian function with the parameters as determined by H1 [4].

As a systematic check, the HERWIG 6.2 [25] model was used to calculate the acceptance correction. The hadronisation stage in HERWIG is described by a cluster fragmentation model [26]. The BE effect is not implemented in the HERWIG model.

6 Systematic uncertainties

The systematic uncertainties of the measured BE correlations were determined by changing the selection cuts or the analysis procedure and repeating the extraction of the BE parameters. The following systematic studies have been carried out, with the resulting uncertainty for the BE radius for the highest-precision measurement (at $Q^2 > 4 \text{ GeV}^2$) given in parentheses:

- the event-selection cuts on y_e , y_{JB} , Z_{vertex} , δ , $E_{e'}$ were varied, and the scattered-lepton energy scale was changed within its uncertainty $\pm 2\%$ ($+0.8\%$ / -0.4%).
- the DA method was used to reconstruct Q^2 and the boost vector to the Breit frame (-0.4%);
- the minimum transverse momentum for tracks was raised by 50 MeV (-3%);

- tracks were required to be within the pseudorapidity range $|\eta| < 1.5$, in addition to the requirement of three CTD superlayers (+0.1%);
- the fit was performed excluding one data point from each side of the region affected by ρ decays. In addition, the lowest Q_{12} bin, which is not well described by the Gaussian parameterisation was excluded from the fit ($^{+0.3\%}_{-0.4\%}$).

The overall systematic uncertainty was determined by adding the above uncertainties in quadrature.

As an additional systematic check, the HERWIG model was used to calculate the acceptance correction. Change in the reconstructed BE radius was +9%. However, HERWIG does not reproduce the measured $\rho(+\!-\!)$ density, so the extraction of the BE effect is less reliable; therefore, this check was not included in the final systematic uncertainties.

Identically charged particles are subject to Coulomb repulsion, which is not simulated by MC models. The Bose-Einstein correlation function was corrected in the data using the Gamow factor [27]. After correcting for the Coulomb effect, the size of the BE radius and λ slightly increased (+4% for r). It was found that this correction does not depend on Q^2 , therefore, it was not included in the final results.

7 Results and discussion

7.1 One-dimensional study

Figure 2 shows the measured $R(Q_{12})$ for $Q^2 > 4 \text{ GeV}^2$ together with the Gaussian fit of Eq. (1) and the exponential fit. The observed distortions for $Q_{12} > 0.9 \text{ GeV}$ are caused by the decay products of resonances which are not well described by the MC simulation. Both parameterisations give fits of similar quality. The extracted parameters for the Gaussian and exponential fits are given in Table 1.

The BE parameters extracted using the Gaussian parameterisation are shown in Fig. 3 as functions of Q^2 . Within the statistical and systematic uncertainties, the data indicate no variations with the virtuality of the exchanged photon in the range $0.1 < Q^2 < 8000 \text{ GeV}^2$ when either the Gaussian or exponential parameterisation is used. This measurement is consistent with an earlier H1 measurement [4] for $6 < Q^2 < 100 \text{ GeV}^2$ using the wrong-charge background subtraction.

Figure 3 also shows the comparisons between the current and the target regions of the Breit frame. The BE effect in the current region was extracted for $Q^2 > 100 \text{ GeV}^2$, where the charged multiplicity is high enough for a reliable measurement. The result indicates

that there is no significant difference between the BE effects in the current and the target regions of the Breit frame. Note that the data shown in Fig. 3 for the total phase space are dominated by the target region.

7.2 Two-dimensional study

The BE correlations can be studied in more than one dimension after decomposing the momentum difference into its transverse and longitudinal components. The BE parameters, r_T , r_L and λ are shown in Figure 4. Table 2 also gives the ratio r_T/r_L . The result shows that the pion-emitting region, as observed in the LCMS, is elongated with r_L being larger than r_T .

Figure 4 and Table 2 also show extracted BE parameters as a function of Q^2 for the two-dimensional measurements. There is again no Q^2 dependence of the BE radii.

7.3 Comparisons with other experiments

One-dimensional BE correlations have been measured in a number of experiments using the wrong-charge background subtraction [28,29,30,31,32,33]. For DIS, the present result agrees well with the μp data at $Q^2 > 4 \text{ GeV}^2$ measured by the EMC Collaboration [28], as well as with the data for $6 < Q^2 < 100 \text{ GeV}^2$ measured by H1 [4], as discussed before.

The data also agree with the LEP1 average $r = 0.78 \pm 0.01(\text{stat.}) \pm 0.16(\text{syst.})$ [34] calculated by combining results for the track-mixing and wrong-charge background-subtraction methods, as well as with LEP2 measurements [30]. The present results also agree with earlier lower-energy e^+e^- annihilation experiments (see a review [35]). Since the BE effect measured in this paper is dominated by the target region, this suggests that the BE effect is not sensitive to the underlying hard processes.

Comparisons with π^+p and pp data [32,31] indicate that the BE radii may be larger for these two processes. However, since the observed BE interference significantly depends on the experimental procedure used to extract the effect, it is difficult to assess quantitative differences between the BE correlations observed in DIS and hadron-hadron collisions.

The measured BE effect reported here disagrees with that in relativistic heavy-ion collisions, which are characterised by significantly larger BE radii, which depend on the atomic number, A , of the projectile as $r \simeq 0.7A^{1/3} \text{ fm}$ [35].

The LEP experiments have recently reported an elongation of the pion source in e^+e^- annihilation events [33]. The present ratio for the two-dimensional BE effect in ep collisions is consistent with these measurements.

8 Conclusions

One- and two-dimensional Bose-Einstein correlations have been studied in deep inelastic ep scattering. The effect was measured as a function of the photon virtuality, Q^2 , in the range from 0.1 to 8000 GeV². The results indicate that the source of identical particles has an elongated shape, consistent with the expectations of the Lund model.

The Bose-Einstein effect in one and two dimensions does not depend on the virtuality of the exchanged photon. The elongation of the pion source is also independent of Q^2 . In addition, the Bose-Einstein correlations in the current and target regions of the Breit frame are similar, even though there is a significant difference in the underlying physics in these two regions.

These high-precision results, obtained over a wide kinematic range in a single experiment, demonstrate that Bose-Einstein interference in ep collisions, and hence the size of the particle-production source, is insensitive to the hard subprocess.

Acknowledgements

We thank the DESY Directorate for their strong support and encouragement. The remarkable achievements of the HERA machine group were essential for the successful completion of this work and are greatly appreciated. We are grateful for the support of the DESY computing and network services. The design, construction and installation of the ZEUS detector have been made possible owing to the ingenuity and effort of many people from DESY and home institutes who are not listed as authors.

References

- [1] G. Goldhaber et al., Phys. Rev. Lett. 3 (1959) 181;
G. Goldhaber et al., Phys. Rev. 120 (1960) 300.
- [2] B. Andersson and W. Hofmann, Phys. Lett. B 169 (1986) 364;
B. Andersson, Acta Phys. Polon. B29 (1998) 1885;
B. Andersson and M. Ringner, Nucl. Phys. B 513 (1998) 627.
- [3] B. Andersson and M. Ringner, Phys. Lett. B 421 (1998) 283.
- [4] H1 Collaboration, C. Adloff et al., Z. Phys. C 75 (1997) 437.
- [5] R.P. Feynman, *Photon-Hadron Interactions*. Benjamin, New York, 1972;
K.H. Streng, T.F. Walsh and P.M. Zerwas, Z. Phys. C 2 (1979) 237.
- [6] ZEUS Collaboration, J. Breitweg et al., Eur. Phys. J. C 11 (1999) 251.
- [7] G. Goldhaber et al., *Proceedings of the Workshop on Local Equilibrium in Strong Interactions (Bad Honnef, West Germany, 1984)*, D.K Scott and R.M. Weiner (eds.), p. 115. World Scientific, Singapore (1985).
- [8] G. Alexander, Rep. Prog. Phys. 66 (2003) 481.
- [9] Csörgő and S. Pratt, *Proceedings of the International Workshop on Relativistic Heavy Ion Physics at Present and Future Accelerators (Budapest 1991)*, T. Csörgő et al. (ed.), p. 75. Budapest, Hungary (1991).
- [10] ZEUS Collaboration, U. Holm (ed.), *The ZEUS Detector*. Status Report (unpublished), DESY (1993), available on <http://www-zeus.desy.de/bluebook/bluebook.html>.
- [11] N. Harnew et al., Nucl. Inst. Meth. A 279 (1989) 290;
B. Foster et al., Nucl. Phys. Proc. Suppl. B 32 (1993) 181;
B. Foster et al., Nucl. Inst. Meth. A 338 (1994) 254.
- [12] M. Derrick et al., Nucl. Inst. Meth. A 309 (1991) 77;
A. Andresen et al., Nucl. Inst. Meth. A 309 (1991) 101;
A. Caldwell et al., Nucl. Inst. Meth. A 321 (1992) 356;
A. Bernstein et al., Nucl. Inst. Meth. A 336 (1993) 23.
- [13] A. Bamberger et al., Nucl. Inst. Meth. A 382 (1996) 419;
S. Magill and S. Chekanov, *Proceedings of the IX International Conference on Calorimetry in High Energy Physics (Annecy, Oct 9-14, 2000)*, B. Aubert et al. (ed.), p. 625. Annecy, France (2001).
- [14] A. Bamberger et al., Nucl. Inst. Meth. A 401 (1997) 63.

- [15] ZEUS Collaboration, J. Breitweg et al., Phys. Lett. B 407 (1997) 432;
ZEUS Collaboration, J. Breitweg et al., Phys. Lett. B 487 (2000) 53.
- [16] S. Bentvelsen, J. Engelen and P. Kooijman, *Proc. Workshop on Physics at HERA*,
W. Buchmüller and G. Ingelman (eds.), Vol. 1, p. 23. Hamburg, Germany, DESY
(1992);
K.C. Höger. Ibid, p.43.
- [17] F. Jacquet and A. Blondel, *Proceedings of the Study for an ep Facility for Europe*,
U. Amaldi (ed.), p. 391. Hamburg, Germany (1979), DESY 79/48.
- [18] H. Abramowicz, A. Caldwell and R. Sinkus, Nucl. Inst. Meth. A 365 (1995) 508.
- [19] L. Lönnblad, Comp. Phys. Comm. 71 (1992) 15.
- [20] A. Kwiatkowski, H. Spiesberger and H.-J. Möhring, Comp. Phys. Comm.
69 (1992) 155.
- [21] H. Spiesberger, HERACLES and DJANGO: *Event Generation for ep Interactions at
HERA Including Radiative Processes*, 1998, available on
<http://www.desy.de/~hspiesb/djangoh.html>.
- [22] R. Brun et al., GEANT3, Technical Report CERN-DD/EE/84-1, CERN, 1987.
- [23] T. Sjöstrand, Comp. Phys. Comm. 82 (1994) 74.
- [24] B. Andersson et al., Phys. Rep. 97 (1983) 31.
- [25] G. Corcella et al., JHEP 0101 (2001) 010.
- [26] B. R. Webber, Nucl. Phys. B 238 (1984) 492;
G. Marchesini and B.R. Webber, Nucl. Phys. B 310 (1988) 461.
- [27] M. Gyulassy, S.K. Kauffmann and L.W. Wilson, Phys. Rev. C 20 (1979) 2267.
- [28] EMC Collaboration, M. Arneodo et al., Z. Phys. C 32 (1986) 1.
- [29] DELPHI Collaboration, P. Abreu et al., Phys. Lett. B 286 (1992) 201;
ALEPH Collaboration, D. Decamp et al., Z. Phys. C 54 (1992) 75;
OPAL Collaboration, G. Alexander et al., Z. Phys. C 72 (1996) 389;
L3 Collaboration, P. Achard et al., Phys. Lett. B 524 (2002) 55;
OPAL Collaboration, G. Abbiendi et al., Phys. Lett. B 559 (2003) 131.
- [30] OPAL Collaboration, G. Abbiendi et al., Eur. Phys. J. C 8 (1999) 559;
L3 Collaboration, M. Acciarri et al., Phys. Lett. B 493 (2000) 233;
L3 Collaboration, P. Achard et al., Phys. Lett. B 547 (2002) 139.
- [31] NA27 Collaboration, M. Aguilar-Benitez et al., Z. Phys. C 54 (1992) 21;
NA22 Collaboration, N.M. Agababyan et al., Z. Phys. C 59 (1993) 195.

- [32] AFS Collaboration, T. Akesson et al., *Z. Phys. C* 36 (1987) 517;
UA1 Collaboration, C. Albajar et al., *Phys. Lett. B* 226 (1989) 410. Erratum-ibid
Phys. Lett. B 229 (1989) 439;
NA23 and EHS-RCBC Collaboration, J.L. Bailly et al., *Z. Phys. C* 43 (1989) 341;
LEBC-EHS and NA27 Collaboration, M. Aguilar-Benitez et al., *Z. Phys.*
C 54 (1992) 21.
- [33] L3 Collaboration, M. Acciarri et al., *Phys. Lett. B* 458 (1999) 517;
DELPHI Collaboration, P. Abreu et al., *Phys. Lett. B* 471 (2000) 460;
OPAL Collaboration, G. Abbiendi et al., *Eur. Phys. J. C* 16 (2000) 423.
- [34] G. Alexander, I. Cohen and E. Levin, *Phys. Lett. B* 452 (1999) 159.
- [35] B. Lörstad, *Int. J. Mod. Phys. A* 4 (1989) 2861.

Q^2 (GeV ²)	λ	r (fm)	λ'	r' (fm)
4 - 8000	$0.475 \pm 0.007^{+0.011}_{-0.003}$	$0.666 \pm 0.009^{+0.022}_{-0.036}$	$0.913 \pm 0.015^{+0.099}_{-0.005}$	$0.928 \pm 0.023^{+0.005}_{-0.094}$
100 - 8000	$0.431 \pm 0.015^{+0.014}_{-0.013}$	$0.646 \pm 0.021^{+0.004}_{-0.029}$	$0.815 \pm 0.037^{+0.110}_{-0.014}$	$0.859 \pm 0.059^{+0.012}_{-0.113}$
0.1 - 1	$0.464 \pm 0.027^{+0.020}_{-0.044}$	$0.602 \pm 0.036^{+0.020}_{-0.051}$	$0.929 \pm 0.069^{+0.076}_{-0.132}$	$0.785 \pm 0.071^{+0.119}_{-0.075}$
4 - 8	$0.468 \pm 0.020^{+0.009}_{-0.006}$	$0.685 \pm 0.028^{+0.004}_{-0.054}$	$0.892 \pm 0.043^{+0.117}_{-0.008}$	$0.954 \pm 0.069^{+0.015}_{-0.168}$
8 - 16	$0.472 \pm 0.016^{+0.029}_{-0.001}$	$0.620 \pm 0.018^{+0.031}_{-0.038}$	$0.911 \pm 0.041^{+0.163}_{-0.004}$	$0.857 \pm 0.054^{+0.040}_{-0.089}$
16 - 32	$0.473 \pm 0.017^{+0.017}_{-0.009}$	$0.629 \pm 0.022^{+0.007}_{-0.035}$	$0.926 \pm 0.052^{+0.174}_{-0.019}$	$0.829 \pm 0.066^{+0.014}_{-0.113}$
32 - 64	$0.496 \pm 0.018^{+0.020}_{-0.013}$	$0.679 \pm 0.022^{+0.022}_{-0.032}$	$0.941 \pm 0.042^{+0.100}_{-0.018}$	$0.910 \pm 0.060^{+0.042}_{-0.076}$
64 - 128	$0.445 \pm 0.017^{+0.019}_{-0.003}$	$0.665 \pm 0.024^{+0.006}_{-0.049}$	$0.843 \pm 0.038^{+0.132}_{-0.007}$	$0.901 \pm 0.063^{+0.006}_{-0.114}$
128 - 400	$0.431 \pm 0.021^{+0.010}_{-0.011}$	$0.649 \pm 0.030^{+0.005}_{-0.036}$	$0.821 \pm 0.050^{+0.087}_{-0.013}$	$0.879 \pm 0.081^{+0.004}_{-0.129}$
400 - 1200	$0.454 \pm 0.059^{+0.005}_{-0.024}$	$0.657 \pm 0.080^{+0.016}_{-0.018}$	$0.852 \pm 0.139^{+0.081}_{-0.019}$	$0.889 \pm 0.216^{+0.027}_{-0.066}$
1200 - 8000	$0.446 \pm 0.120^{+0.063}_{-0.086}$	$0.837 \pm 0.164^{+0.117}_{-0.073}$	$0.841 \pm 0.234^{+0.132}_{-0.173}$	$1.227 \pm 0.389^{+0.237}_{-0.169}$

Table 1: *The values of the one-dimensional BE parameters for different Q^2 ranges. The Gaussian and exponential parameterisations were used to extract the parameters. The statistical and systematic uncertainties are indicated.*

Q^2 (GeV ²)	λ	r_L (fm)	r_T (fm)	r_T/r_L
4 - 8000	$0.44 \pm 0.01^{+0.01}_{-0.03}$	$0.95 \pm 0.03^{+0.03}_{-0.08}$	$0.69 \pm 0.01^{+0.01}_{-0.06}$	$0.72 \pm 0.03^{+0.04}_{-0.03}$
100 - 8000	$0.32 \pm 0.03^{+0.02}_{-0.01}$	$0.88 \pm 0.08^{+0.03}_{-0.06}$	$0.62 \pm 0.04^{+0.05}_{-0.01}$	$0.70 \pm 0.08^{+0.06}_{-0.01}$
0.1 - 1	$0.41 \pm 0.05^{+0.08}_{-0.00}$	$0.82 \pm 0.09^{+0.03}_{-0.02}$	$0.74 \pm 0.08^{+0.01}_{-0.13}$	$0.91 \pm 0.14^{+0.03}_{-0.18}$
4 - 16	$0.46 \pm 0.02^{+0.06}_{-0.01}$	$0.84 \pm 0.04^{+0.04}_{-0.03}$	$0.69 \pm 0.02^{+0.04}_{-0.02}$	$0.83 \pm 0.05^{+0.03}_{-0.00}$
16 - 64	$0.39 \pm 0.02^{+0.03}_{-0.05}$	$1.03 \pm 0.07^{+0.20}_{-0.11}$	$0.66 \pm 0.03^{+0.02}_{-0.02}$	$0.64 \pm 0.05^{+0.07}_{-0.10}$
64 - 400	$0.34 \pm 0.02^{+0.02}_{-0.05}$	$0.85 \pm 0.07^{+0.21}_{-0.05}$	$0.62 \pm 0.03^{+0.03}_{-0.00}$	$0.73 \pm 0.07^{+0.06}_{-0.16}$
400 - 8000	$0.42 \pm 0.10^{+0.06}_{-0.01}$	$1.08 \pm 0.27^{+0.12}_{-0.00}$	$0.67 \pm 0.11^{+0.11}_{-0.03}$	$0.62 \pm 0.18^{+0.07}_{-0.05}$

Table 2: *The values of the two-dimensional BE parameters for different Q^2 ranges, as well as the ratio r_T/r_L . The Gaussian parameterisation was used to extract the parameters. The statistical and systematic uncertainties are indicated.*

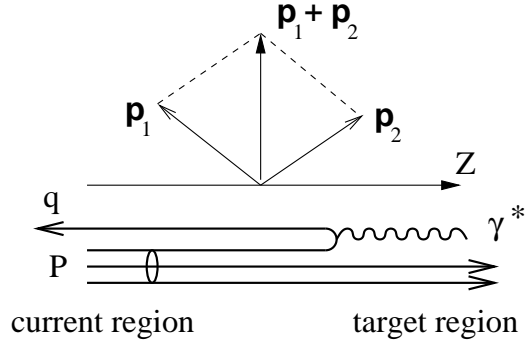


Figure 1: *The longitudinally co-moving system for a pair of particles in DIS. This system is defined as the frame of reference in which the sum of the two-particle momenta, \mathbf{p}_1 and \mathbf{p}_2 , is perpendicular to the γ^*q axis, which coincides with the Z axis of the Breit frame.*

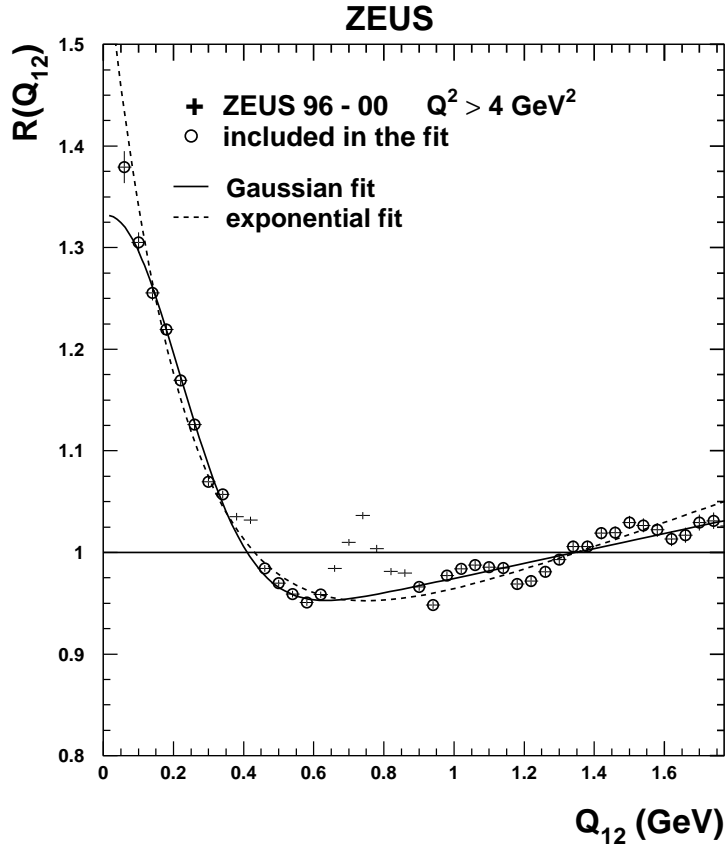


Figure 2: *The measured Bose-Einstein correlation function, $R(Q_{12})$, together with the Gaussian and the exponential fits. The error bars show the statistical uncertainties. The data points included in the fit are marked with the circles.*

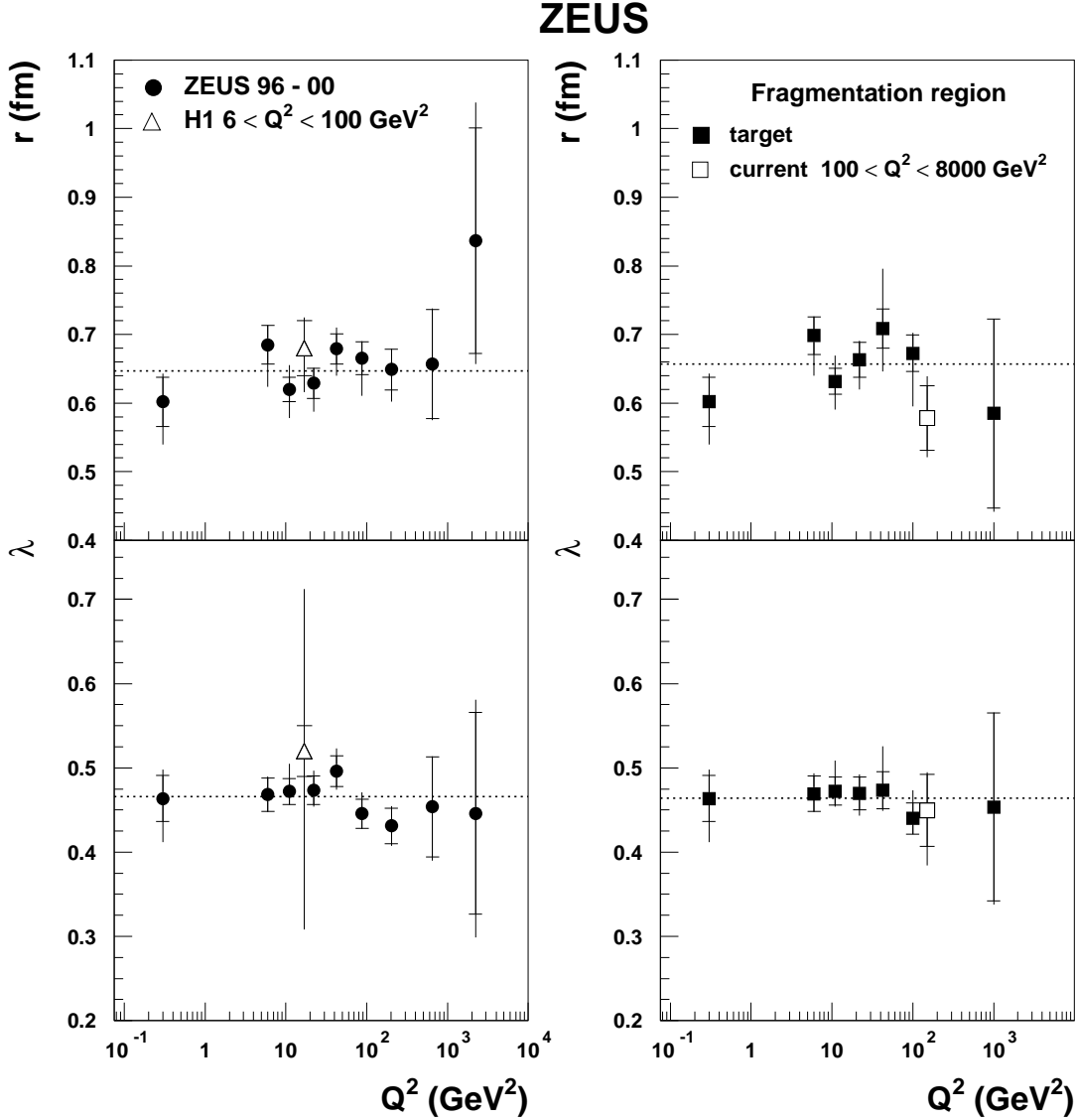


Figure 3: *The extracted radius, r , and the incoherence parameter, λ , as functions of Q^2 for the total measured phase space (left figures) and for the target region and the current region of the Breit frame (right figures). The H1 data point is shown for the mean value of the measured Q^2 range, $6 < Q^2 < 100$ GeV 2 . The BE effect is shown for the current fragmentation region for $100 < Q^2 < 8000$ GeV 2 . The inner error bars are statistical uncertainties; the outer are statistical and systematic uncertainties added in quadrature. The dotted lines show the average values, with the $\chi^2/ndf \simeq 0.5$ for both r and λ .*

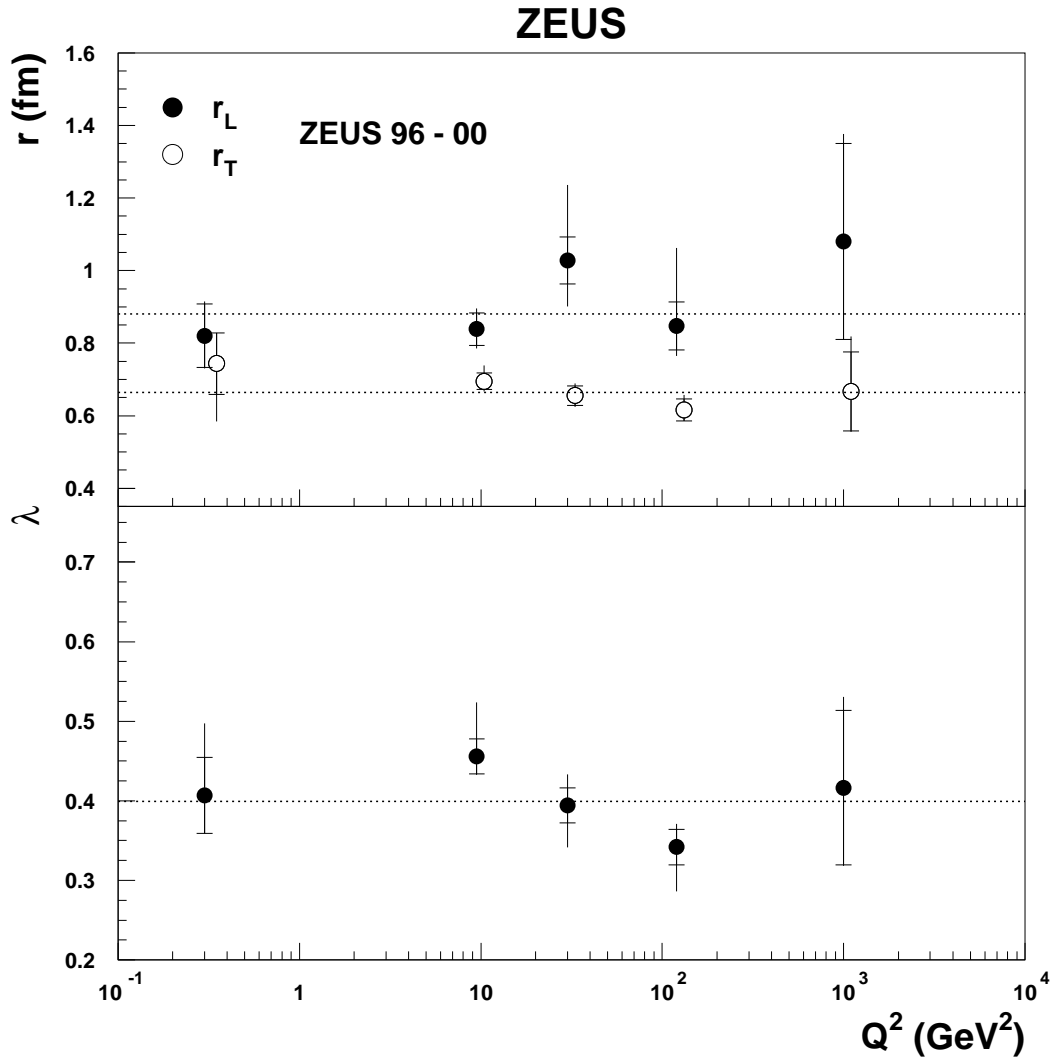


Figure 4: *The extracted radii, r_T , r_L , and the incoherence parameter λ as functions of Q^2 for the two-dimensional correlation function $R(Q_T, Q_L)$. The inner error bars are statistical uncertainties; the outer are statistical and systematic uncertainties added in quadrature. The dotted lines show the average values.*